

The effects of neutron irradiation on the physicommechanical properties of refractory metals*

Maria I. Zakharova¹, Vladimir P. Tarasikov¹

¹ JSC “SSC RF – IPPE” n.a. A.I. Leypunsky, 1 Bondarenko Square, 249033 Obninsk, Kaluga Region, Russia

Corresponding author: Vladimir P. Tarasikov (vptarasikov@mail.ru)

Academic editor: Yury Kazansky ♦ **Received** 31 October 2019 ♦ **Accepted** 18 April 2020 ♦ **Published** 25 June 2020

Citation: Zakharova MI, Tarasikov VP (2020) The effects of neutron irradiation on the physicommechanical properties of refractory metals. Nuclear Energy and Technology 6(2): 117–123. <https://doi.org/10.3897/nucet.6.55230>

Abstract

Studying the interaction of radiation defects with defects in the crystal lattice in the initial state makes it possible to distinguish the contribution of each type of defect to changes in the physicommechanical properties of materials exposed to irradiation. When comparing the changes in the properties of the metals with the body-centered cubic (BCC) lattice (Mo, W, V, Nb) and hexagonal close-packed (HCP) lattice (Re), we see common features and differences in their behavior under irradiation:

- both HCP and BCC crystals show an orientation dependence of their properties; at the same time, the metals with the BCC lattice are characterized by an increase in the size of the sample in all crystallographic directions, whereas, for the HCP crystals, the sample is narrowed along the $\langle 0001 \rangle$ direction, perpendicular to the plane with the closest packing of atoms, and expanded along other directions;
- for the BCC samples, the elastic moduli decrease; for the HCP samples, the shear modulus increases significantly as a result of irradiation;
- electrical resistance for the metals of Group 6 (Mo, W) and rhenium as a result of irradiation increases; for the metals of Group 5 (V, Nb), it decreases: this decrease in electrical resistance is associated with the release of interstitial impurity atoms to radiation defects;
- for the BCC crystals, relaxation processes occur both in the unirradiated and irradiated samples, whereas, in the HCP crystals, only irradiation and post-irradiation annealing cause the temperature dependence of internal friction (TDIF) and the appearance of a relaxation maximum due to a change in the point symmetry of the defect; and
- during isochronous annealings up to $0.7 \times T_m$, behavior features associated with the crystal lattice structure are retained.

Keywords

Neutron irradiation, refractory metals, molybdenum, tungsten, vanadium, niobium, rhenium, radiation defects, impurity atoms, electrical resistance, internal friction, elastic moduli, radiation swelling

* Russian text published: Izvestiya vuzov. Yadernaya Energetika (ISSN 0204-3327), 2020, n. 1, pp. 78–88.

Introduction

Studying the effects of neutron irradiation on the physico-mechanical properties of refractory metals and related alloys occupies one of the leading places in radiation material science (Neklyudov et al. 2014, Koryukin and Churin 2017, Zakharova and Tarasikov 2018, Blanter et al. 2017).

Single crystals of refractory metals are a convenient object for studying the stability of crystal lattices as well as the interaction of radiation defects with interstitial and substitutional impurity atoms in a wide temperature range. In addition, they are used in facilities for direct conversion of nuclear power into electricity as cathode and anode materials (Koryukin and Churin 2017).

Materials and experimental conditions

The test materials were metals with the BCC lattice (molybdenum, tungsten, vanadium, and niobium) and with the HCP lattice (rhenium). The samples were cut from single-crystal zone melting rods in the form of rectangular prisms $1.5 \times 1.5 \times 22$ mm in size, the axis of the sample corresponded to one of the crystallographic directions, i.e., $\langle 100 \rangle$, $\langle 110 \rangle$ or $\langle 111 \rangle$ for the BCC lattice and $\langle 0001 \rangle$ for the HCP lattice. The deviation of the crystallographic axis from the sample axis did not exceed 4° , the dislocation density was no more than $2 \times 10^{10} \text{ m}^{-2}$, the sub-grain boundary angles were $30''$ – $30'$ for molybdenum and tungsten, and 1° for vanadium, niobium, and rhenium. The samples were irradiated in the BR-10 reactor core up to a fluence of $1.14 \times 10^{26} \text{ n/m}^2$ ($E > 0.1 \text{ MeV}$) at a temperature of 460°C in hermetically sealed fuel element tubes. Post-irradiation annealing of the irradiated samples was carried out isochronously with the samples as witnesses in containers made of the same materials in a vacuum of $1.33 \times 10^{-3} \text{ Pa}$ in the temperature range of 300 – 1700°C through 100°C for one hour.

The low-frequency internal friction and elastic moduli were determined by the torsion pendulum method in the amplitude-independent region (Birzhevoy et al. 2019) up to 600°C with an error of no more than 2%. The electrical resistance was measured by the potentiometric method with an error of 1% for room temperature and 3.5% for nitrogen temperature. The radiation swelling was evaluated by changing the size of the samples with an error of 0.01%.

Results and discussion

Changes in the physico-mechanical properties under irradiation

Changes in the physico-mechanical properties of molybdenum, tungsten, niobium, vanadium and rhenium as a result of irradiation are presented in Tab. 1.

Table 1. Changes in the properties of the refractory metals as a result of neutron irradiation ($1.14 \times 10^{26} \text{ n/m}^2$, $E > 0.1 \text{ MeV}$, 460°C).

Material	Electrical resistance, $\Delta\rho/\rho$, %		Shear modulus, $\Delta G/G$, %	Young's modulus, $\Delta E/E$, %	Length, $\Delta L/L$, %	Volume, $\Delta V/V$, %
	25 °C	-196 °C				
Molybdenum	$\langle 100 \rangle$	14	111	-11	-8	–
	$\langle 110 \rangle$	10	92	-9	-10	–
	$\langle 111 \rangle$	12	94	-6	-12	–
Tungsten	$\langle 100 \rangle$	17	128	-2	-2	0.32
	$\langle 110 \rangle$	14	114	-2	-2	0.25
	$\langle 111 \rangle$	14	102	-4	-8	0.16
Niobium	$\langle 100 \rangle$	-6	-21	-11	-14	1.1
	$\langle 110 \rangle$	0	-4	-9	-13	1.05
	$\langle 111 \rangle$	1	-10	-8	-12	0.65
Vanadium	$\langle 100 \rangle$	-4	-9	-9	-8	0.90
Rhenium	$\langle 0001 \rangle$	6	31	32	–	-0.55

Changes in the transverse dimensions a_1 and a_2 of the rhenium samples as a result of irradiation are as follows: $\Delta a_1/a_1 = 0.88$, $\Delta a_2/a_2 = 0.41$.

As can be seen in the table, the changes in the properties of the metals with the BCC and HCP lattices are different in nature. In the metals with the BCC lattice, the elastic moduli decrease in all crystallographic directions; in the metals with the HCP lattice, they increase. The smallest changes in the elastic moduli are observed in tungsten (Zakharova et al. 2001). In molybdenum and niobium, the maximum changes in the shear modulus are manifested for the $\langle 100 \rangle$ orientation.

In molybdenum, tungsten (Group 6) and rhenium, the electrical resistance increases due to irradiation; in vanadium and niobium (Group 5), it decreases. The maximum changes in the electrical resistance correspond to the $\langle 100 \rangle$ orientation. Changes in the dimensions of the samples under irradiation also depend on the orientation. For all the metals with the BCC lattice, these values are positive; for rhenium, the size of the sample decreases by 0.55 % along the $\langle 0001 \rangle$ direction and increases along the other faces (a_1 and a_2). The nature of the change in the dimensions of the samples under irradiation correlates with the magnitude of the swelling.

Recovery of the properties during isochronous annealings

Figure 1 shows the specific electrical resistance recovery curves of the molybdenum and vanadium samples during isochronous annealings. For different crystallographic orientations of the molybdenum samples, the character of the electrical resistance recovery is identical. However, the onset of annealing of the electrical resistance increment for the samples with the $\langle 111 \rangle$ orientation is shifted by approximately 200°C towards higher temperatures. It should be noted that the electrical resistance completely recovers only after $0.7T_m$ is reached, which is associated with the accumulation of niobium and zirconium in molybdenum due to nuclear reactions.

The electrical resistance recovery for the metals of Group 6 is shown by the example of vanadium (Fig. 1b). As can be seen in the figure, the level of changes in the

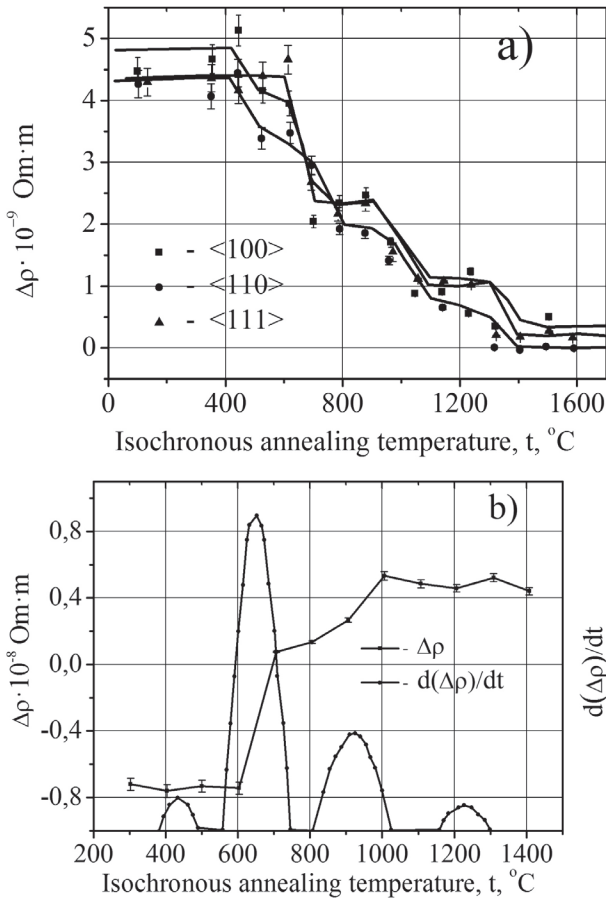


Figure 1. Recovery of the electrical resistance of the irradiated samples of molybdenum (a) and vanadium (b) during isochronous annealing.

electrical resistance caused by irradiation is maintained up to 600 °C, then, there is an increase up to $0.7T_m$. There is no complete electrical resistance recovery to be observed in this temperature range, and this can also be associated with the accumulation of transmutant’s (chromium, titanium) (Zakharova et al. 2001). The changes under irradiation and the recovery during annealing of the electrical resistance specific for the metals of Groups V and VI are due to different solubilities of interstitial impurities in the lattices of these metals.

Figure 2 shows the temperature dependences of the internal friction and the resonance frequency of torsional vibrations (shear modulus) of unirradiated and irradiated niobium with the orientation of the sample axis along the $\langle 111 \rangle$ direction.

On Internal Friction Curve 1, two relaxation peaks are observed at temperatures of 180 and 325 °C. The activation energy of the processes corresponding to the peaks at 180 and 325 °C was calculated by the formula taken from (Birzhevoy et al. 2019). The activation energy is 1.17 eV for the first peak and 1.52 eV for the second peak, respectively, which corresponds to the migration energies of oxygen and nitrogen atoms in the niobium lattice. After irradiation in the niobium samples of all the orientations under study, the oxygen peak disappears, the height of the

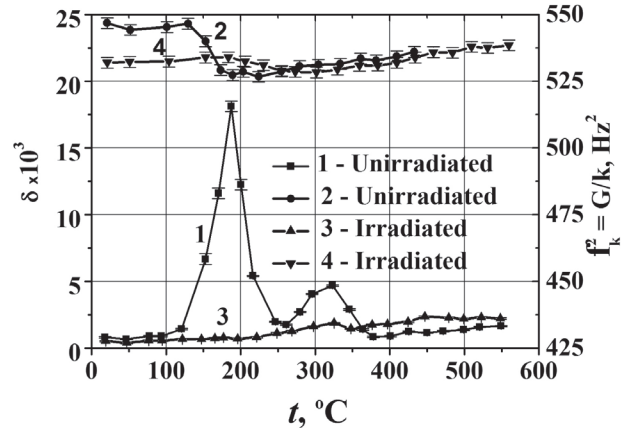


Figure 2. Temperature dependences of internal friction Δ (1, 3) and the square of the frequency of torsional vibrations f_k^2 (2, 4) of the unirradiated (Curves 1, 2) and irradiated (Curves 3, 4) niobium samples with the $\langle 111 \rangle$ orientation.

nitrogen peak decreases significantly and a wide diffuse peak appears (Curve 3). A similar picture is observed for vanadium (Zakharova and Tarasikov 2018).

In the BCC crystals, inelastic relaxation (Snoek relaxation) is caused by interstitial atoms (oxygen, nitrogen, carbon) located in octahedral and tetrahedral interstices. The point symmetry of this position of the interstitial atoms is tetragonal, which is lower than the cubic symmetry of the crystal. The Snoek peak height is proportional to the concentration of interstitial atoms in the solid solution and is sensitive to various types of exposure, including irradiation with nuclear particles. Consequently, the decrease or disappearance of relaxation peaks during irradiation can be associated with the release of interstitial atoms from the positions of introduction of the crystal lattice to radiation defects with the formation of complex set. Curves 2 and 4 show a decrease in the shear modulus of the irradiated sample as compared with the unirradiated one, and in the region of existence of the relaxation peaks, the softening of the lattice occurs (i.e., the modulus defect appears). The decrease in the elastic moduli during irradiation can also be associated with the release of impurity element atoms from the solid solution. Similar processes occur in metals of Group 6 as well.

On the curve of the temperature dependence of internal friction (TDIF) for rhenium (Fig. 3), in the temperature range of 25–600 °C, no changes are observed up to an annealing temperature of 900 °C. Starting from 1000 °C the TDIF is manifested, which is clearly formed at 1300 °C and increases as the annealing temperature rises up to 1500 °C. As the annealing temperature rises, the rise of the curve shifts towards lower temperatures. The TDIF is not manifested in the non-irradiated samples, since individual point (intrinsic and impurity) defects in the HCP crystals cause mainly strains with the trigonal symmetry. Such defects (elastic dipoles) are aligned along the c -axis, and they do not cause dissipation of elastic energy. The observed increase in internal friction in the irradiated rhenium crystals is apparently

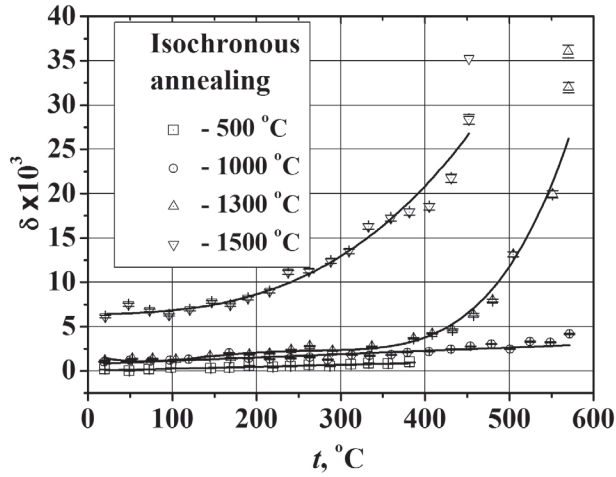


Figure 3. Temperature dependence of internal friction Δ of irradiated rhenium for various isochronous annealing temperatures.

the beginning of a relaxation peak that can occur in the irradiated samples due to the appearance of new defects with a decrease in the point symmetry of the defect relative to its location in the matrix.

Shown in Fig. 3, the dependences of internal friction of irradiated rhenium for various isochronous annealing temperatures can be described by the following expressions:

- for 500 °C with a standard error of 0.1×10^3

$$\Delta = (0.035 + 0.00223t) \times 10^3; \quad (1)$$

- for 1000 °C with a standard error of 0.39×10^3

$$\Delta = (0.645 + 0.00443t) \times 10^3; \quad (2)$$

- for 1300 °C with a standard error of 1.77×10^3

$$\Delta = (3.745 - 0.0955t + 9.0875 \times 10^{-4}t^2 - 2.9566 \times 10^{-6}t^3 + 3.1731 \times 10^{-9}t^4) \times 10^3; \quad (3)$$

- for 1500 °C with a standard error of 2.18×10^3

$$\Delta = (5.054 + 0.039t - 2.112 \times 10^{-4}t^2 + 5.374 \times 10^{-7}t^3) \times 10^3, \quad (4)$$

where Δ is the internal friction; t is the measurement temperature, °C.

As was shown earlier by the example of metals with the BCC lattice, complex aggregates of radiation defects are formed in irradiated crystals with the participation of interstitial atoms. Similar processes can also occur under irradiation in the HCP crystals. Relaxation peaks from the oxygen atom – substitutional atom pair were observed in hafnium and titanium, which also have the HCP lattice. This interpretation of the TDIF is consistent with the shear modulus temperature behavior (see Fig. 4) – in the region where the relaxation peak is formed (see Fig. 3), the shear modulus is clearly reduced at the same isochronous annealing temperatures.

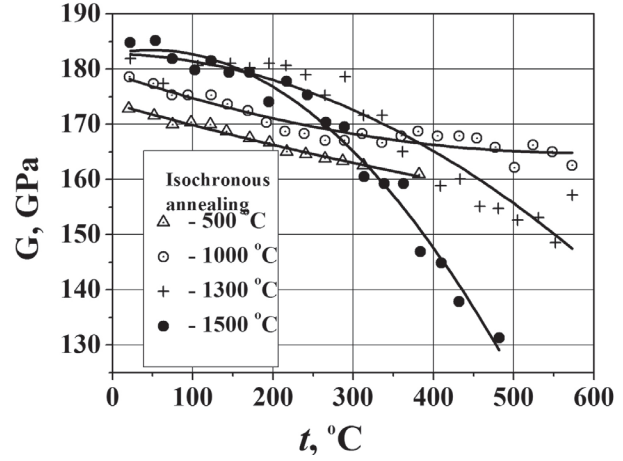


Figure 4. Temperature dependence of the shear modulus G of irradiated rhenium for various isochronous annealing temperatures.

Shown in Fig. 4, the dependences of the shear modulus of irradiated rhenium for various isochronous annealing temperatures can be described by the following expressions:

- for 500 °C with a standard error of 0.5 GPa

$$G = 173.8 - 0.041t + 1.58 \times 10^{-5}t^2; \quad (5)$$

- for 1000 °C with a standard error of 1.5 GPa

$$G = 179.2 - 0.049t + 4.16 \times 10^{-5}t^2; \quad (6)$$

- for 1300 °C with a standard error of 3.8 GPa

$$G = 182.8 - 0.0033t - 1.018 \times 10^{-4}t^2; \quad (7)$$

- for 1500 °C with a standard error of 2.6 GPa

$$G = 182.8 + 0.028t - 2.895 \times 10^{-4}t^2, \quad (8)$$

where G is the shear modulus, GPa; t is the measurement temperature, °C.

The TDIF of the niobium samples with the orientation of the sample axes along the $\langle 111 \rangle$ direction for a number of isochronous annealing temperatures is shown in Fig. 5a. When annealed at temperatures from 300 to 700 °C, the second peak grows and the third peak shifts towards higher temperatures. The growth of the second peak ends at 800 °C, and it does not transform afterwards. The third peak grows to an annealing temperature of 700 °C, and in the temperature range from 800 to 1000 °C it completely disappears. Starting from 800 °C, the oxygen peak manifests itself and sharply increases, its growth mainly ends at a temperature of 1000 °C, and the third peak completely disappears at the same temperature. Further up to 1700 °C, the oxygen peak grows at a lower rate.

Figure 5b shows the temperature dependence of the shear modulus G of the niobium samples (the $\langle 111 \rangle$ orientation) for various isochronous annealing temperatures. As the relaxation peak grows, the modulus defect increases.

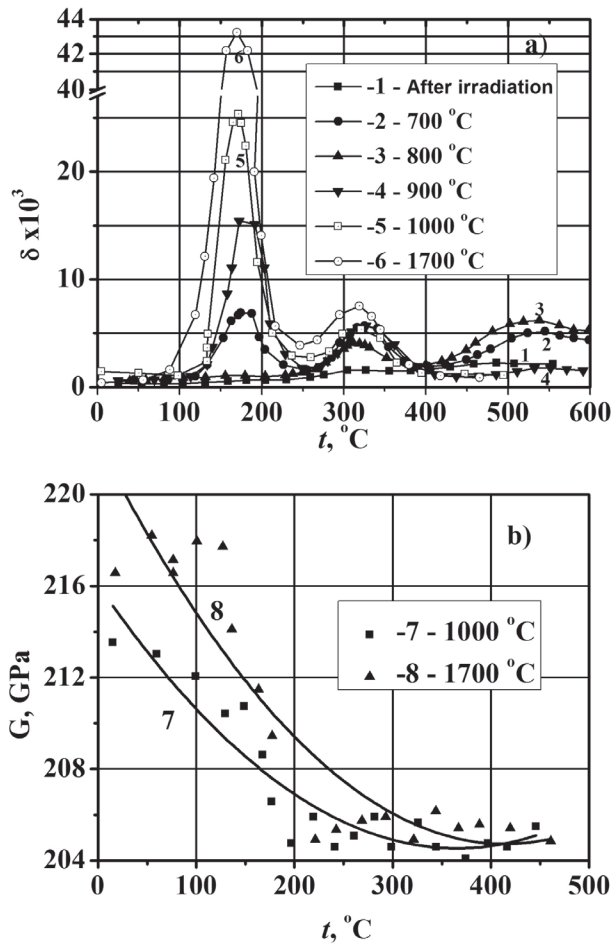


Figure 5. Dependences of the parameters of niobium samples with the $\langle 111 \rangle$ orientation on isochronous annealing temperatures: a) – internal friction Δ ; b) – shear modulus G .

An analysis of the internal friction spectrum recovery in niobium during isochronous annealing shows that the main contribution to the formation of complex radiation complexes is made by oxygen atoms. The activation energy of annealing of defects corresponding to the third peak is 1.73 eV. Then, taking into account the activation energy of the migration of oxygen atoms (1.17 eV), the binding energy of the complex aggregate will be 0.56 eV. In vanadium, the internal friction recovery during isochronous annealing proceeds in a similar way (Zakharova and Tarasikov 2018).

A comparison of the recovery curves of the spectrum of internal friction and electrical resistance shows that, in vanadium, the first group of defects is detected only by the return of the electrical resistance with activation energy of 1.56 eV. The recovery of properties in the range of 480–850 °C proceeds with an activation energy of 1.68 eV. Taking into account the fact that the Snoek peak returns to the position corresponding to the oxygen peak, one can assume that at this stage the oxygen – radiation defect aggregates break and oxygen atoms migrate in the crystal lattice interstitial position. The activation energy of the migration of oxygen atoms in vanadium is 1.26 eV; therefore, the binding energy of the complex aggregate is 0.42 eV. In the range of 820–1200 °C further recovery of

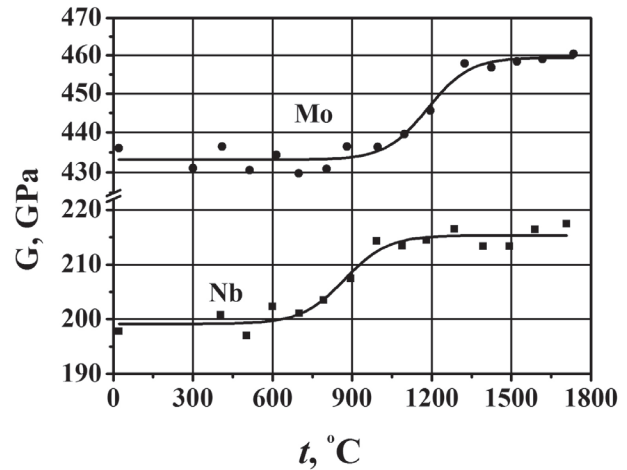


Figure 6. Dependence of the shear modulus of the irradiated niobium and molybdenum samples on the isochronous annealing temperature.

the Snoek peak occurs and a nitrogen peak appears. The activation energy of this process is 2.12 eV. The activation energy of the migration of nitrogen atoms is 1.47 eV; hence the binding energy of the nitrogen – radiation defect aggregate is 0.65 eV.

Figures 6, 7 show the recovery curves of the shear moduli during isochronous annealings in niobium, molybdenum and rhenium. An analysis of these dependences shows a stepwise recovery of the moduli in the BCC crystals upon isochronous annealing of the irradiated samples (see Fig. 6) while, for the HCP crystals (rhenium), the temperature dependence of the shear modulus behaves differently (see Fig. 7). After irradiation, as noted earlier, the shear modulus of the rhenium samples increases from 125 to 164 GPa.

Shown in Fig. 6, the dependences of the shear modulus of the irradiated niobium and molybdenum samples on the isochronous annealing temperature can be described by the following expressions:

- for niobium with a standard error of 1.8 GPa

$$G = 215.3 - 16.16 / (1 + \exp((t - 870.75) / 81.59)); \quad (9)$$

- for molybdenum with a standard error of 2.4 GPa

$$G = 459.5 - 26.28 / (1 + \exp((t - 1186.62) / 78.96)), \quad (10)$$

where G is the shear modulus, GPa; t is the isochronous annealing temperature, °C.

Shown in Fig. 7, the dependence of the shear modulus of the irradiated rhenium samples on the isochronous annealing temperature can be described by the following expression:

$$G = 171.7 + 0.031t - 1.51 \times 10^{-5}t^2, \quad (11)$$

where G is the shear modulus, GPa; t is the isochronous annealing temperature, °C.

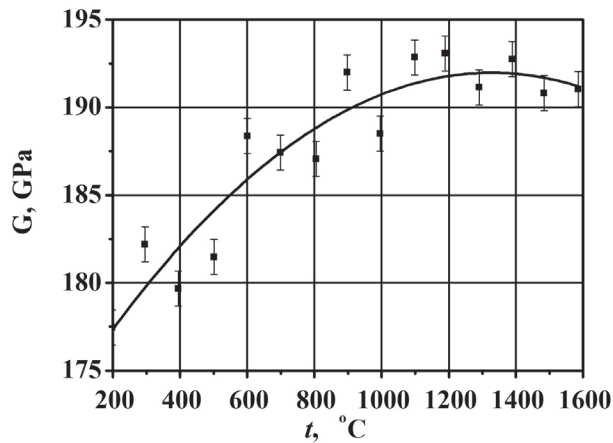


Figure 7. Dependence of the shear modulus of the irradiated rhenium samples on the isochronous annealing temperature.

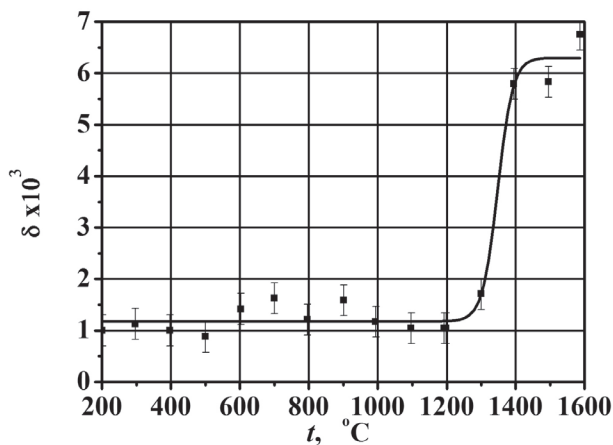


Figure 8. Dependence of internal friction of the irradiated rhenium samples on the isochronous annealing temperature.

In addition, irradiation of both the BCC and HCP crystals leads to a decrease in the internal friction background compared to the initial values, which indicates a significant decrease in the mobility of various defects during irradiation and, for rhenium, a decrease in the internal friction background occurs by more than an order of magnitude.

For rhenium, during isochronous annealing up to 1100 °C, the shear modulus additionally grows relative to the modulus of the irradiated sample before annealing. With a further increase in the temperature, the shear modulus practically does not change. Although, as can be seen in Fig. 8, in the temperature range of 1300–1600 °C, the TDIF is observed. This behavior of the shear modulus, taking into account the appearance of the TDIF, which is not observed

in the initial samples, indicates that upon irradiation and post-irradiation annealing of the HCP crystals, the defect structure is rearranged in them with the participation of impurity atoms, which leads to a change in the point symmetry of the defect with respect to the matrix symmetry.

Shown in Fig. 8 the dependence of internal friction of the irradiated rhenium samples on the isochronous annealing temperature with a standard error of 0.3×10^3 can be described by the following expression:

$$\Delta = (6.30 - 5.12 / (1 + \exp(t - 1347) / 21.86)) \times 10^3, \quad (12)$$

where Δ is the internal friction; t is the isochronous annealing temperature, °C.

Conclusions

When comparing the changes in the properties of metals with the BCC lattice and HCP lattice, we can see common features and differences in their behavior under irradiation:

- both the HCP and BCC crystals show an orientation dependence of their properties; at the same time, the metals with the BCC lattice are characterized by an increase in the size of the sample in all crystallographic directions, whereas, for the HCP crystals, the sample is narrowed along the $\langle 0001 \rangle$ direction, perpendicular to the plane with the closest packing of atoms, and expanded along other directions;
- for the metals with the BCC lattice, the elastic moduli decrease; for the sample with the HCP lattice, the shear modulus increases significantly as a result of irradiation;
- the electrical resistance for the metals of Group 6 (Mo, W) and rhenium as a result of irradiation increases; for the metals of Group 5 (V, Nb), it decreases: this decrease in electrical resistance is associated with the release of impurity interstitial atoms to radiation defects;
- for the BCC crystals, relaxation processes occur both in the unirradiated and irradiated samples, whereas, in the HCP crystals, only irradiation and post-irradiation annealing cause the TDIF and the appearance of a relaxation maximum due to a change in the point symmetry of the defect; and
- during isochronous annealings up to $0.7T_m$, behavior features associated with the crystal lattice structure are retained.

References

- Birzhevoy GA, Zakharova MI, Tarasikov VP (2019) Formation of aggregates of interstitial – substitutional atoms in ferritic-martensitic steel EP-823 for various types of heat treatment VANT. Series: Material Science and New Materials 2 (98): 4–11.
- Blanter MS, Dmitriev VV, Mogutnov BM, Ruban AV (2017) Interaction of Interstitial Atoms and Configurational Contribution to their Thermodynamic Activity in V, Nb and Ta. Physics of Metals and Metal Science, 118(2): 111–118. <https://doi.org/10.1134/S0031918X17020016>

- Koryukin VA, Churin VA (2017) Diffusion and Thermal Emission of Mo-W Emitters of Power Generating Channels. VANT. Series: Physics of Nuclear Reactors, 5: 79–86.
- Neklyudov IM, Voevodin VN, Laptev IN, Parkhomenko AA (2014) On the Effects of Irradiation on the Elastic Moduli of Metallic Materials. VANT. Series: Physics of Radiation Damage and Radiation Material Science 2(90): 21–28.
- Zakharova MI, Artemov NA, Bogdanov VV (2001) The effects of neutron irradiation and annealing on the elastic moduli and electrical resistance of single crystals of molybdenum and tungsten. Inorganic Materials 37(8): 931–935. <https://doi.org/10.1023/A:1017979230262>
- Zakharova MI, Tarasikov VP (2018) Thermal stability of radiation effects in single-crystal vanadium. VANT. Series: Material Science and New Materials 4(95): 4–15.